Characterization of spray-coating methods for conjugated polymer blend thin films

Noebels, Matthias; Cross, Rachel Elizabeth; Evans, D. A.; Finlayson, Christopher

Published in:
Journal of Materials Science

DOI:
10.1007/s10853-014-8123-5

Publication date:
2014

Citation for published version (APA):
Noebels, M., Cross, R. E., Evans, D. A., & Finlayson, C. (2014). Characterization of spray-coating methods for conjugated polymer blend thin films. *Journal of Materials Science*, *49*(12), 4279-4287. https://doi.org/10.1007/s10853-014-8123-5

Characterization of spray-coating methods for conjugated polymer blend thin-films

Matthias Noebels, Rachel E. Cross, D.A. Evans and Chris E. Finlayson

Institute of Mathematics, Physics & Computer Science (IMPACS), Prifysgol Aberystwyth University, Aberystwyth, Wales SY23 3BZ, United Kingdom.

e-mail: cef2@aber.ac.uk
Tel: 0044 1970 622818

Abstract – We examine the characteristics and functionality of conjugated polymer thin-films, based on blends of poly(9,9-dioctylfluorene-2,7-diyl-co-bis-N,NN´-(4-butylphenyl)-bis-N,N´-phenyl-1,4-phenylenediamine) (PFB) and poly(9,9-dioctylfluorene-2,7-diyl-co benzothiadiazole)(F8BT), using a spray-coating deposition technique suitable for large areas. The morphological properties of these blend films are studied in detail by Atomic Force Microscopy (AFM) methods, showing that favourable results, in terms of layer deposition rate and uniformity, can be achieved using a 5:1 blend of o-dichlorobenzene and chlorobenzene as the solvent medium. A photoluminescence quenching efficiency of above 80% is also observed in such blend films. As a feasibility study, prototypical photovoltaic devices exhibit open circuit voltages of up to 1.0V under testing, and solar power conversion efficiencies in the 0.1-1% order of magnitude; metrics which are comparable with those reported for spin-coated cells of the same active blend and device architecture.

Keywords – Polymer blends, Polymer films, Conjugated Polymers, Deposition methods, Structures

INTRODUCTION

Large-area mass production techniques for organic optoelectronics, such as solar photovoltaic cells and LEDs, still represent a significant scientific and engineering challenge. In most cases, polymer electronic devices are laminar, which means that the molecules are printed or otherwise applied as thin films on foils or surfaces; spin-coating is perhaps the easiest and best studied route to producing efficient organic solar cells at the present [1]. This opens a wide field of applications, such as displays [2], electronic paper [3] or photovoltaic systems [4]. However, because of its different character, new manufacturing processes have to be developed, though techniques originally invented for printing or painting can be advanced. A current research area is, for example, the use of screen printing in order to produce photovoltaic devices [5].

Here, we explore spray-coating via conventional airbrush equipment as a possible production technology for bulk-heterojunction organic photovoltaic (OPV) cells. Further to recent reports on Fullerene-based cells by Susanna *et al*., Lidzey *et al*. and others [6], we study all-polymer (polymer-polymer) OPVs. In particular, the influence of key experimental parameters on layer deposition rate and uniformity, the detailed thin-film morphology (characterizing the roughness of films, the nature of the "coffee-stain" structures, the nature of any micron-scale phase separation), and the photophysical properties of the blend system (e.g. photoluminescence quenching). Furthermore, the steps to produce prototypical photovoltaic devices using spray-coating are described and the devices are characterized and compared.

The morphological properties of these F8BT/PFB blend films are studied in detail by Atomic Force Microscopy (AFM), showing that favourable results, in terms of layer deposition rate and uniformity, can be achieved using a 5:1 blend of o-dichlorobenzene and chlorobenzene as the solvent medium. A photoluminescence quenching efficiency of above 80% is also observed in such blend films. The resulting devices exhibit open circuit voltages of up to 1.0 V under testing, and solar power conversion efficiencies in the range of 0.1-1%; metrics which are comparable with those reported for spin-coated OPVs of the same active layer and device architecture [7]. Importantly, the spray-coating methods described here are highly scalable in nature, in a way that techniques such as spin-coating and vacuum deposition are not; hence, offering a genuinely different engineering paradigm.

EXPERIMENTAL

Spray coating of polymer blends

When prehistoric man invented the first airbrush by using reed or hollowed bones for their cave paintings, they already realized the capability of uniform and large-area colour layers in comparison to finger or brush paintings. Although this technology has been developed a lot since those ancient times, the basic principle is still the same; air with a certain pressure is

used to nebulize paint and accelerates the droplets towards a surface. The paint itself can basically be any liquid and therefore also solutions of dissolved polymers used for organic optoelectronics.

For the spray-coating experiments a double-action, siphon-feed airbrush gun type 128 produced by Wiltec was used. The airbrush has a working pressure range from 1 to 3.4 bar and a nozzle diameter of 0.35 mm. Double-action refers to the feature that a single lever is used to control both air pressure and paint flow rate. Furthermore, the airbrush is siphon-feed, which means that the solution is drawn by the air pressure from a cup underneath the gun.

Following on from literature reports of suitable solvents [7,8], o-Dichlorobenzene (DCB), chlorobenzene (CB) and toluene (all from Sigma-Aldrich) are used for this work. All parts of the airbrush are known to be resistant against these solvents. The conjugated polymers used in the preparation of photovoltaic blends, namely poly(9,9-dioctylfluorene-2,7-diyl-co-bis-N,NN´-(4-butylphenyl)-bis-N,N´-phenyl-1,4 phenylene-diamine) (PFB) and poly(9,9-dioctylfluorene-2,7-diyl-cobenzothiadiazole) (F8BT) were obtained from Cambridge Display Technology Ltd,[1] and are illustrated in Figure 1.

Working Principle

A schematic view of the airbrush and spray-coating set-up is depicted in Figure 1. The basic working principles of an airbrush relies both on Bernoulli's principle, which states that an increase in the speed of a gas or fluid causes a decrease in pressure, and the nebulization of liquids by an increase in surface energy. Significant for the size of the droplets produced by nebulization is the mass flow ratio between the pressurized gas and the solution passing the mixing point. A higher ratio leads to smaller droplets; this can be regulated via a lever on the gun. Compressed gas from a gas bottle or compressor enters the airbrush through a valve opened by pressing the lever. The gas passes a bottleneck, which leads to an increase in speed. The reduction in air pressure caused by the propelled gas draws the solution out of the cup and to the mixing point, which is at the tip of the gun needle. At this point the nebulization of the paint takes place, as the surface energy of the solvent increases, producing small droplets.

Initially, the influences of the different parameters as the spraying process have to be studied, in order to allow production of regular, uniform, and reproducible films. Relevant parameters are the nozzle-substrate distance (see Fig.1), the gas pressure, the flow rate and the substrate temperature. In these reports, compressed nitrogen gas (N_2) is used to supply the airbrush. Early experiments with liquid propellants showed that the air stream coming out of the airbrush also contains small amounts of the propellant, which can lead to an unwanted transfer of propellant onto the substrate.

Distance and Pressure

[1] These materials were characterized as follows- F8BT; Mn = 81k, Mp = 174k, polydispersity (PD) = 2.6, photoluminescence quantum-yield (PLQY) = 82%. PFB; Mn = 39k, Mp = 162k, PD = 4.5, PLQY = 27%.

The effects of the nozzle-substrate distance (d) and the air pressure (p) are significantly interdependent. On the one hand, a minimum air pressure is necessary to allow the nebulization of the polymer solution. Using a higher pressure also decreases the size of the droplets, which leads to a more regular film. However, if the air pressure is too high, the droplets will be blown away once they hit the substrate, leading to a non-contiguous "splatter" pattern. A greater nozzle-substrate distance prevents this, but increases the area covered by the airbrush and will therefore lead to a higher wastage of material. Furthermore, a short distance leads to a wet, irregular film, whereas a too high distance leads to a dry, dusty film, because the solvent droplets evaporate on their way to the substrate. By numerous trial runs, an ideal distance of d = 17 cm with an N_2 pressure of p = 1.4 bar was empirically determined.

Flow rate and Film Formation

In order to increase the reproducibility of the sprayed films, the air pressure was regulated directly at the gas bottle, so that the airbrush lever is only used to adjust the solvent rate. The actual flow rates were typically 10s of microlitres per second using a gas pressure of p = 1.4 bar, with a correlation between the viscosity of a solvent (see Table 1) and the flow rate. A relatively volatile solvent such as toluene facilitates suction and the jet formation during the spraying process and leads to a higher flow rate. On the other hand, a viscous solvent like DCB leads to a lower flow rate. By adding a less viscous component (i.e. CB), the flow rate may be increased again.

When selecting a suitable flow rate for spray-coating, it has to be considered that a higher flow rate reduces the required spray duration, but also increases the droplet sizes, which leads to a more irregular film. In order to solve this problem, the process of film formation on the substrate has to be first considered. As soon as a droplet hits the substrate, the solvent evaporates and leaves the dissolved polymer material behind. The evaporation process of a droplet is difficult to describe, depending on many parameters, but it is essentially based on equilibrium between the liquid phase of the droplet itself and the surrounding vapor phase. A good way to therefore control the drying time is the temperature, since higher temperatures accelerate the evaporation process. The minimum temperature required for a film consisting of single and independent droplets depends on the flow rate and the boiling point of the solvent (see Table 1). In a test experiment, the substrate was heated on a thermostat-controlled hot plate and the minimum temperature necessary for an immediately dry substrate after a spray duration of 10 seconds was determined (see Table 1). Again, toluene with the lowest boiling point requires the lowest temperature, and DCB with the highest boiling point, the highest temperature. By adding a fraction of CB the minimum temperature decreases slightly.

Film thickness

The thickness of the resulting thin-film is dependent on the solvent, the polymer concentration and the spray duration. To rationalize the potential number of experimental

parameters, the polymer blend has been fixed to a 1:1 mass ratio of PFB:F8BT and an overall polymer concentration of 5 mg ml^{-1}, hence in the approximate range used in refs 7 and 8. The hot plate was set to the corresponding substrate temperatures shown in table 1. In order to comply with the standardizations in the previous section, the substrates were sprayed on in intervals of 10 seconds, and after each interval the substrates were dried for 30 seconds. We observe an almost proportional relationship between spray duration and layer thickness, as measured using absorbance spectroscopy and then by comparison with extinction co-efficients from the literature [9], showing that new layers are actually sprayed on top of previous layers instead of only dissolving them. No significant effects of de-wetting of the deposited layers were observed. Table 1 shows the resulting film thickness deposition rates for the solvent media used in this study.

Importantly, UV-vis absorption characterisation of these films indicates that the desired 1:1 ratio of the blend components is retained in the coating process (see Fig. 1d). Indeed, the extinction coefficients at around 400 and 470 nm, associated with PFB and F8BT respectively, are matched for all the thicknesses studied.

The photomicrographs of spray-coated films in Figure 2 show similar structural characteristics for each of the different solvent media used; films made of dried droplets with typical sizes of 10s of microns. Based on the size of these "coffee stain" structures and the rapid evaporation of the drops upon impact, we can estimate droplet sizes of 10-25 μm with DCB:CB as the solvent medium and 20-50 μm with toluene. This would be consistent with a so-called *fine atomisation* regime from comparable literature reports involving direct Phase Doppler measurements.[10] For all solvents, the overlap of several droplets and almost no combining of droplets into larger ones is clearly visible. A more detailed analysis, using AFM measurements, is reported in the *Results* section.

Photovoltaic device preparation

It had been found that thick layers with little loss of material and moderate substrate temperatures can be achieved using a 5:1 mixture by volume of DCB and CB, hence this solvent medium was use in the production of prototypical solar cells (see Figure 1c), with all other spraying parameters maintained as previously described.

The quartz glass substrates were pre-coated with an ITO layer (from Psiotec). The PEDOT:PSS layer is deposited via spin-coating; for this, PEDOT:PSS (Sigma-Aldrich) is diluted 1:2 in deionized water. 25 μl of solution is applied onto the substrate, before spin-coating for 50 seconds at around 5,500 rpm. Afterwards the PEDOT:PSS layer is annealed and baked under inert nitrogen flow at 230°C for 30 minutes. Because of the hygroscopic character of PEDOT:PSS, the F8BT:PSS active layer was then deposited by spraying within an hour. The Aluminum electrode is thermally evaporated using an Edwards E306 evaporator, evacuated to a pressure of less than 2×10^{-5} mBar. Devices are then immediately legged, using standard metal cramps, in preparation for electrical testing. Whilst the working area of these devices was limited to 0.64 cm^2 by the area of the ITO substrates used, it should

be noted that we were readily able to evenly coat much larger substrate areas of up to 10s of cm^2 with the sprayed active layer.

The output characteristics of the produced solar cells were examined within a home-made "dark box". The cells were mounted on a sample holder inside the box. The light from a 50 Watt (max) halogen lamp outside the box, powered by a regulated Kenwood PD35-10 power supply, was shone through a close-able shutter onto the cell. The distance between light source and sample holder was fixed at 10 cm, and the measured light flux onto the device was 1,600 lux, at a measured colour temperature of ~3,000 K. The entire area of the devices (as defined by the electrode overlap area) was uniformly illuminated. The cells were connected to a Keithley 6430 sub-femtoamp remote source meter via a remote pre-amplifier, in order to record the I-V characteristics of devices.

RESULTS

Polymer Blend Morphology

Atomic force micrographs (AFM) of 1:1 F8BT/PFB films, as spray-coated from various solvent media (DCB, toluene, and DCB:CB 5:1), are shown in Figure 2. These measurements confirm that films are made of dried droplets with typical sizes of 10-50 μm. When projected in a 3D relief view, the AFM images show "coffee-stain" structures with walls and flat centres, as shown in Figure 3. In all three cases, the flat centres show a good flatness uniformity; typically with height variation of only a few nm, as shown in the line height-profiles. However, the coffee-stain walls give more pronounced height variation. In the blends sprayed from DCB/DCB:CB the walls may be up to 10 microns wide and 100 nm high; for toluene, walls appear less pronounced with widths of a few microns and heights of 20-40 nm. Commensurately, it can be seen from Table 2 that the films sprayed from toluene have a rather lower roughness, as analyzed over a representative 40 x 40 μm area. In all case, the film coverage appears to be complete, with few gaps between the droplets being in evidence.

These micrographs show no obvious large-scale phase separation of blend components, in a fashion which is similar with comparable spin-coated films using chlorinated solvents (e.g. chloroform), but in contrast to those spun from (e.g.) xylene [11]. Upon focusing the AFM measurements onto smaller (100 x 100 nm) areas, using specially designed low frequency tips for soft matter samples (ND-MDT, Scanwel Ltd), we observe some nanoscale structure. Figure 4 shows a micrograph taken on an area within a droplet centre, and indicates some evidence of directional structuring. This may be a phenomenon associated with the radial flow of material as droplets are deposited on the substrate and then spread outwards, as the solvent is rapidly removed. The effect such nano-structuring would have on the functioning of such a photovoltaic blend is unclear, and this issue merits future

investigation, possibly with the use of Kelvin Probe scanning microscopy, in order to resolve the different components of the polymer blend in terms of their electronic states [12].

Photoluminescence Quenching

In their pristine state, the polyfluorenes generally exhibit a high luminescence quantum yield efficiency, when photoexcited [13]. The fluorescence intensity can be decreased by quenching processes, for example by internal conversion or energy/charge transfer of the excited state to other molecules (quenchers). This is particularly interesting for photovoltaic devices, as such a quenching of the photoluminescence is indicative of the ionisation of electron-hole pairs at heterojunction interfaces; these carriers do not recombine if the charges are extracted from the device, and they therefore do not generally re- emit a photon. Hence, we expect that the photoluminescence of a solar cell decreases with an increasing charge separation efficiency; so we can thus calculate the photoluminescence quenching (PLQ) efficiency, which reveals how efficiently electron-hole pairs are separated and charge carriers are extracted from the devices without recombination. The PLQ can be simply defined by the ratio of dissociated electron-hole pairs to the number of photons absorbed by the material. In order to account for the other non-radiative pathways available to the photo-generated pairs (excitions), this measurement is then referenced to the emission from a pristine F8BT film of known quantum yield efficiency and absorption cross-section.

The PLQ efficiencies of several spray-coated films, based on different solvents and spray durations, were examined. The devices were made of a 1:1 blend of PFB and F8BT with a polymer concentration of 5 mg ml^{-1} in either toluene, DCB or a 5:1 blend of DCB and CB. The solutions were sprayed on quartz glass substrates in 1, 2 or 3 intervals of 10 seconds duration, as before. A film made of F8BT only, with a concentration of 2.5 mg ml^{-1} in a 5:1 DCB:CB blend, was used as reference. A standard experimental setup for measuring the PL/PLQ efficiency was used [14], with a 488 nm Argon ion laser source of a few mW used to excite the samples. Because the absorption of F8BT is much higher at a wavelength of 488 nm than that of PFB, we can thus use the pristine F8BT-only film as our reference standard and treat PFB as the quenching agent.

The PLQ efficiencies for blends sprayed from the 3 solvent media, for a range of optically inferred film thicknesses, are shown in Table 3. We expect differences in the degree of PL quenching using different solvents, because the blend micro-/nano-structures should depend on the film formation and the characteristics of the solvent; the length-scale of the phase separation between PFB and F8BT and its comparison to exciton diffusion lengths, being of particular importance to charge separation efficiency. However, we would have expected that the PLQ should not critically depend on the film thickness. The results in fact show some random variation with thickness, whereas the solvent medium seems less critical, suggesting no significant changes in the phase separation between PFB and F8BT. McNeill *et al*. [15], report a PLQ of 0.95 for spin-coated devices based on PFB and F8BT without annealing and a decrease of PLQ to 0.70 for devices annealed at 160°C. Considering that the

spray-coated devices were produced at temperatures of up to 100°C, thus resembling an annealing step, the PL quenching of spin-coated and spray-coated devices is similar.

Photovoltaic Cell Performance

Typical I-V characteristics for prototypical photovoltaic cells are given for a range of active layer thicknesses in Figure 5. The measured open circuit voltages (V_{oc}) for the produced devices are in the range of 0.5 to 1.0 V, showing a generalized trend of increasing V_{oc} with increasing thickness, as inferred in Figure 5c . It is expected that V_{oc} will be influenced by the nature of the electrodes, but not usually by the layer thickness. In particular, there may be sensitivity to slight variations in the ambient conditions (temperature, relative humidity etc.) during the active-layer deposition.

The short circuit current I_{sc} of devices are also displayed in Figure 5c, as functions of active layer thickness. The I_{sc} values can be normalized to a short circuit current density Jsc by dividing by the size of the active area (in our case 64 mm^2); this gives J_{sc} values in the range of 1 to 5 $\mu A/cm^2$. In an idealized bulk heterojunction system [16], I_{sc} should increase with an increasing layer thickness, as the optical absorption and exciton generation rate rises. However, I_{sc} should decrease again for large thicknesses, because of the longer transport distances of charge carriers to the electrodes. In the present case, there is a general trend for I_{sc} to increase quite sharply with decreasing thickness, down to the thinnest measured devices (~ 50 nm), which is likely indicative of relatively short carrier transport lengths within the active layer. Calculating the series resistance of cells by the usual method ($V > V_{oc}$ regime) yields values in the range of 1 - 10 $k\Omega.cm^2$ (taking device area into account), and fill-factors (as usually defined, derived from figure 5b) are typically of order 0.3 to 0.4; both of these indicators imply a limit to the absolute power conversion efficiencies achievable with the present design and layer-deposition protocols.

To ascertain the performance of these prototypical OPVs, the power conversion efficiency η, which is defined as $\eta = P_{MaxPowerPoint}/P_{Incident\ Light}$, was calculated in each case. Correction is also made for the light source being of a lower colour temperature than the standard photopic function as provided by the International Commission on Illumination (CIE) [17]. The average value of η, over >10 samples, was 0.12%, with the highest measured value being 0.25%. We can make a comparison with the spin-coated devices of McNeill et al., where η values of around 1% have been previously reported in F8BT:PFB and 1.5-2% in alternative blend systems such as polythiophenes/poly(phenylene-vinylenes) [7,15]. It should be noted that these values are also limited by the non-ideal matching of the lamp spectrum to the F8BT/PFB action spectrum, which is predominantly in the blue/green end of the visible.

Without illumination, a photovoltaic cell should behave like a normal rectifying diode; enabling cells in reverse bias to operate as photodetectors, as long as the dark current is not too high [18]. However, film morphology has been previously shown to have an influence on the dark current behavior of organic solar cells. For example, Green *et al.* [8],

describe the negative effect of roughness and pinholes between the contacts on the dark current behavior, and an increase for smoother and annealed devices. For unstressed devices, measured in the dark-box as before, dark current densities are in the range of 100 nA/cm^2. The measurements suggest a dependence of the dark current on the layer roughness, because spray-coated devices show higher reverse leakage currents than analogous spin-coated ones. Additionally, devices which were annealed after depositing the active layer for 10 minutes at 180°C, usually exhibited a slightly reduced reverse leakage current.

A final issue to consider is the stability/longevity of devices in their present ambient conditions and un-encapsulated state. Current-voltage characteristics of the best-performing spray-coated OPVs were re-measured after a period of 7 days after production. Typically, a decrease in I_{sc} and maximum power by factors of up to 5 were observed. Similar behavior was experienced by K. Kawano *et al*. [19], when they examined the degradation of MDMO-PPV: PCBM solar cells with and without PEDOT:PSS layer as a function of atmospheric conditions. They describe the water absorption of PEDOT:PSS due to its hygroscopic character, producing inhomogeneities and the formation of insulating patches in the planar devices.

DISCUSSION

Whilst the performance metrics of the OPV devices reported here approach the same order of magnitude as that reported for spin-coated cells of the same active blend and device architecture, they are clearly significantly below that of many state-of-the-art organic solar cell exemplars from the literature [20]. It is anticipated that better control of the environmental factors of production and storage would give better, more stable devices than the prototypes described here. Also, the relatively low-cost and high-availability of the polyfluorenes make them attractive for this kind of exploratory work on developing spray-coated polymer blend films. Applying this knowledge towards the use of advanced low-bandgap materials would allow spray-coated OPVs with better solar spectral matching properties to be exploited.

An interesting comparison may also be drawn with recent reports of OPV cell fabrication using inkjet-based technologies [21]. Indeed, the typical characteristics of the final films, such as the size of deposited droplets and the levels of surface roughness, are somewhat comparable. Both of these technologies offer some advantages, as viable alternatives to spin-coating for optoelectronics applications [5]. Inkjet certainly offers a route to structures not accessible with spin coating, such as patterned grids or electrodes; whereas for very high material throughput (whilst still achieving reduced material loss) and large-area deposition, spray-coating is likely to be the more favorable of the two methods. Indeed, such pros-and-cons might also be considered to exist in comparison with other state of the art film forming methods for OPVs, such as roll-to-roll printing methods. [22]

As a future direction of this work, we are currently examining the possibilities of using the related "electro-spraying" method [23] for depositing OPV active layers. This is another reported method of deposition for thin films, which also enables the deposition of delicate and fragile molecules, in a precise and controllable fashion, in both atmosphere and vacuum. One could envisage multilayers (thickness-dependent compositions) of "small molecule" film-forming semiconductors; such as PCBM or oligomeric donors [24], with whole new regimes of polymer blend morphology are possible, as compared with spin-coating or Langmuir-Blodgett techniques. In both conventional spray-coated and electrospraying, the very rapid solvent removal will allow compositional control, but with better ordered structures than the amorphous forms typical of traditional vacuum-sublimation materials used in organic electronics, such as the oligo-acenes [25].

CONCLUSIONS

A spray-coating method has been employed in the production of all-polymer (polyfluorene) blend thin-films. Detailed studies of the influence of key experimental parameters on layer deposition rate and uniformity, the detailed thin-film morphology (including AFM) studies characterizing the roughness of films, the nature of the "coffee-stain" structures, the nature of any micron-scale phase separation (or lack thereof), and the photophysical properties of the blend system (e.g. photoluminescence quenching), are reported. These characterizations of the deposited blend films show them to be of suitable characteristics for potential use in photovoltaic cells. As an important feasibility step, the resulting prototypical photovoltaic devices exhibit open circuit voltages of up to 1.0V under testing, and solar power conversion efficiencies in the 0.1-1% order of magnitude range; metrics which are comparable with key analogues reported using methods of spin-coating for the active layer deposition. In the light of this, and of other very recent reports, [26] we propose that such spray-coating methods hold great potential as an approach to the challenges presented by the scale-up and large area mass fabrication of OPVs.

ACKNOWLEDGEMENTS

The authors thank Mr Matt Gunn of Aberystwyth University for advice and technical assistance. The authors acknowledge Cambridge Display Technology (CDT Ltd) for the supply of materials used in this work, and Scanwel Ltd for technical support with AFM measurements. This work was supported by a Royal Society (UK) *Research Grant* (RG110313).

REFERENCES

[1] Middleman S, Hochberg AK (1993) Process Engineering Analysis in Semiconductor Device Fabrication. McGraw-Hill, New York

[2] Kamtekar KT, Monkman AP and Bryce MR (2010) Recent Advances in White Organic Light-Emitting Materials and Devices, Adv Mater 22:572-582.

[3] Gelinck GH, Huitema HEA, van Veenendaal E et al (2004) Flexible active-matrix displays and shift registers based on solution-processed organic transistors, Nature Mater 3:106-110.

[4] Günes S, Neugebauer H and Sariciftci NS (2007) Conjugated polymer-based organic solar cells, Chem Rev 107:1324-1338; Bouclé J, Ravirajan P and Nelson J (2007) Hybrid polymer–metal oxide thin films for photovoltaic applications, J Mater Chem 17:3141-3153; Thompson BC and Fréchet JMJ (2008) Organic photovoltaics: Polymer-fullerene composite solar cells, Angew Chem Intl Ed 47:58-77; Chen H-Y, Hou J, Zhang S et al (2009) Polymer solar cells with enhanced open-circuit voltage and efficiency, Nature Photonics 3:649-653; Jørgensen M, Norrman K and Krebs FC (2008) Stability/degradation of polymer solar cells, Sol Energy Mater Sol Cells 92:686-714.

[5] Krebs FC (2009) Fabrication and processing of polymer solar cells: a review of printing and coating techniques, Sol Energy Mater Sol Cells 93:394-412.

[6] Susanna G, Salamandra L, Brown TM, Di Carlo A, Brunetti F and Reale A (2011) Airbrush spray-coating of polymer bulk-heterojunction solar cells, Sol Energy Mater Sol Cells 95:1775-1778; Abdellah A, Fabel B, Lugli P and Scarpa G (2010) Spray deposition of organic semiconducting thin-films: Towards the fabrication of arbitrary shaped organic electronic devices, Organic Electronics 11:1031–1038; Girotto C, Rand BP, Genoe J and Heremans P (2009) Exploring spray coating as a deposition technique for the fabrication of solution-processed solar cells, Sol Energy Mater Sol Cells 93:454–458; Hoth CN, Steim R, Schilinsky P, Choulis SA, Tedde SF, Hayden O and Brabec CJ (2009) Topographical and morphological aspects of spray coated organic photovoltaics, Organic Electronics 10:587–593

[7] McNeill CR and Greenham NC (2009) Conjugated-Polymer Blends for Optoelectronics, Adv Mater 21:3840-3850.

[8] Green R, Morfa A, Ferguson AJ, Kopidakis N, Rumbles G and Shaheen SE (2008) Performance of bulk heterojunction photovoltaic devices prepared by airbrush spray deposition, Appl Phys Lett 92:033301.

[9] Shikler R and Friend RH (2007) Modeling the effect of the structure of polymer photocells on their absorption spectrum, J Appl Phys 102:013105.

[10] Mueller R and Kleinebudde1 P (2007) Comparison of a Laboratory and a Production Coating Spray Gun With Respect to Scale-up, AAPS Pharm Sci Tech 8(1):E1-E11.

[11] Kietzke T (2007) Recent Advances in Organic Solar Cells, Advances in OptoElectronics article ID 40285.

[12] Hallam T, Lee M, Zhao N, Nandhakumar I, Kemerink M, Heeney M, McCulloch I and Sirringhaus H (2009) Local Charge Trapping in Conjugated Polymers Resolved by Scanning Kelvin Probe Microscopy, Phys Rev Lett 103:256803.

[13] Mullen K and Scherf U (2006) Organic Light-Emitting Devices. John Wiley & Sons, USA

[14] Finlayson CE and Whitney AD (2010) Photophysical studies of poly-isocyanopeptide based photovoltaic blends, J Phys D: Applied Physics 43:095501.

[15] McNeill CR, Westenhoff S, Groves C, Friend RH and Greenham NC (2007) Influence of Nanoscale Phase Separation on the Charge Generation Dynamics and Photovoltaic Performance of Conjugated Polymer Blends: Balancing Charge Generation and Separation, J Phys Chem C 111:19153-19160.

[16] Moulé AJ, Bonekamp JB and Meerholz K (2006) The effect of active layer thickness and composition on the performance of bulk-heterojunction solar cells, J Appl Phys 100:094503.

[17] Commission Internationale de l'Eclairage (CIE) proceedings of 1931 (1932). Cambridge University Press, UK

[18] Menke SM, Pandey R and Holmes RJ (2012) Tandem organic photodetectors with tunable, broadband response, Appl Phys Lett 101:223301.

[19] Kawano K, Pacios P, Poplavskyy D, Nelson J, Bradley DDC and Durrant JR (2006) Degradation of organic solar cells due to air exposure, Sol Energy Mater Sol Cells 90:3520-3530.

[20] Liang YY, Xu Z, Xia J, Tsai S-T, Wu Y, Li G, Ray C and Yu L (2010) For the bright future-bulk heterojunction polymer solar cells with power conversion efficiency of 7.4%, Adv Mater 22:E135–E138; Yuan Y, Huang J and Li G (2011) Intermediate Layers in Tandem Organic Solar Cells, Green 1:65-80.

[21] Lange A, Wegener M, Fischer B, Janietz S and Wedel A (2012) Solar Cells with Inkjet Printed Polymer Layers, Energy Procedia 31:150-158; Hoth CN, Schilinsky P, Choulis SA and Brabec CJ (2008) Printing Highly Efficient Organic Solar Cells, Nano Lett 8:2806–2813.

[22] Søndergaard RR, Hösel M and Krebs FC (2012) Roll-to-Roll fabrication of large area functional organic materials, J Poly Sci B: Polymer Physics 51:16-34; Søndergaard RR, Hösel M, Angmo D, Larsen-Olsen TT and Krebs FC (2012) Roll-to-roll fabrication of polymer solar cells, Materials Today 15:36-49; Frederik C. KrebsKrebs FC, Espinosa N, Hösel M, Søndergaard RR and Jørgensen M (2014) Rise to Power – OPV-Based Solar Parks, Adv Mater 26:29-39.

[23] Jaworek A (2007) Electrospray droplet sources for thin film deposition, J. Mater. Sci. 42:266-297; Muhammad NM, Sundharam S, Dang H-W, Lee A, Ryu B-H and Choi K-H (2011) CIS layer deposition through electrospray process for solar cell fabrication, Current Applied Physics 11:S68-S75.

[24] Sun Y, Welch GC, Leong W-L, Takacs CJ, Bazan GC and Heeger AJ (2012) Solution-processed small-molecule solar cells with 6.7% efficiency, Nature Mater 11:44-48.

[25] Tang ML, Reichardt AD, Nobuyuki M, Stoltenberg RM and Bao Z (2008) Ambipolar, High Performance, Acene-Based Organic Thin Film Transistors, J Am Chem Soc 130:6064-6065.

[26] Wang T, Scarratt NW, Yi H et al (2013) Fabricating High Performance, Donor-Acceptor Copolymer Solar Cells by Spray-Coating in Air, Adv Energy Mater 3:515-512.

TABLES

TABLE 1 Key parameters for solvent media used in spray-coating of 5 mg/ml F8BT:PFB blend

	Viscosity η (cP)	Boiling point (°C)	Minimum substrate T (°C)	Deposition rate (nm/sec)
Toluene	0.59	110	20	3.4
DCB	1.32	180	100	4.1
DCB:CB 5:1	1.22	< 180	80	5.1

[a] Viscosity for mixed solvents calculated using Refutas equation.

TABLE 2 Sample roughness, as derived from area analysis of AFM

	Roughness (peak-to-valley, nm)	Roughness (standard deviation, nm)	Average Roughness (nm)
DCB:CB 5:1	79.8	18.5	15.8
Toluene	62.0	17.4	14.7
DCB	77.1	22.1	19.1

TABLE 3 Photoluminescence quenching (PLQ) efficiency of spray-coated 1:1 F8BT/PFB blends

Solvent	Film thickness (nm)	PLQ
DCB:CB 5:1	75	0.70 ± 0.11
	105	0.55 ± 0.11
	155	0.64 ± 0.05
Toluene	40	0.57 ± 0.14
	60	0.85 ± 0.09
	105	0.76 ± 0.16
DCB	60	0.63 ± 0.18
	105	0.75 ± 0.08
	135	0.67 ± 0.17

FIGURE CAPTIONS

Figure 1. (a) Schematic of the pneumatically driven ejection mechanism ("spray gun") used. A double-action, siphon-feed spray gun (Wiltec type 128) was used, with working pressure range 1.0-3.4 bar and nozzle diameter 0.35 mm. (b) Chemical structure of conjugated semiconducting polymers PFB and F8BT, as indicated. (c) Schematic of laminar photovoltaic cell design, with working area 0.64 cm^2. (d) UV-vis spectra (absolute absorbance vs. wavelength) of spray-coated F8BT/PFB blends of several deposition thicknesses, as indicated. For comparison, spectra of pristine F8BT and PFB films (of ≈ 100 nm thickness) are also shown on the same axes/scale.

Figure 2. (left) Optical micrographs of spray-coated 1:1 F8BT/PFB films from solvent media (a) DCB:CB 5:1, (b) toluene, and (c) DCB. The images were taken with a 40x objective, NA = 0.65. (right) Corresponding 40 x 40 μm atomic force micrographs (AFM), with the height scales in nanometers given in each case.

Figure 3. Atomic force micrographs (AFM), as shown in 3D relief view, for spray-coated films from solvent media (a) DCB:CB 5:1, (b) toluene, and (c) DCB. (right) Illustrative line height-profiles are shown below for each micrograph.

Figure 4. 100 x 100 nm AFM, as shown in 3D relief view, in droplet centres for spray-coated 1:1 F8BT/PFB films from DCB:CB 5:1. This shows some evidence of directional structuring.

Figure 5. (a) Full I-V characteristics of representative spray-coated solar cells under illumination at 1,600 lux. Data are presented on an absolute log scale graph, and the thicknesses of the active layers are as indicated. (b) Corresponding data showing behavior within the quadrant defined by short-circuit current (I_{sc}) and open-circuit voltage (V_{oc}). (c) The variation of I_{sc} (circles) and V_{oc} (crosses) as a function of active-layer thickness. Linear trendlines are added as a visual aid.

Figure 1
Click here to download high resolution image

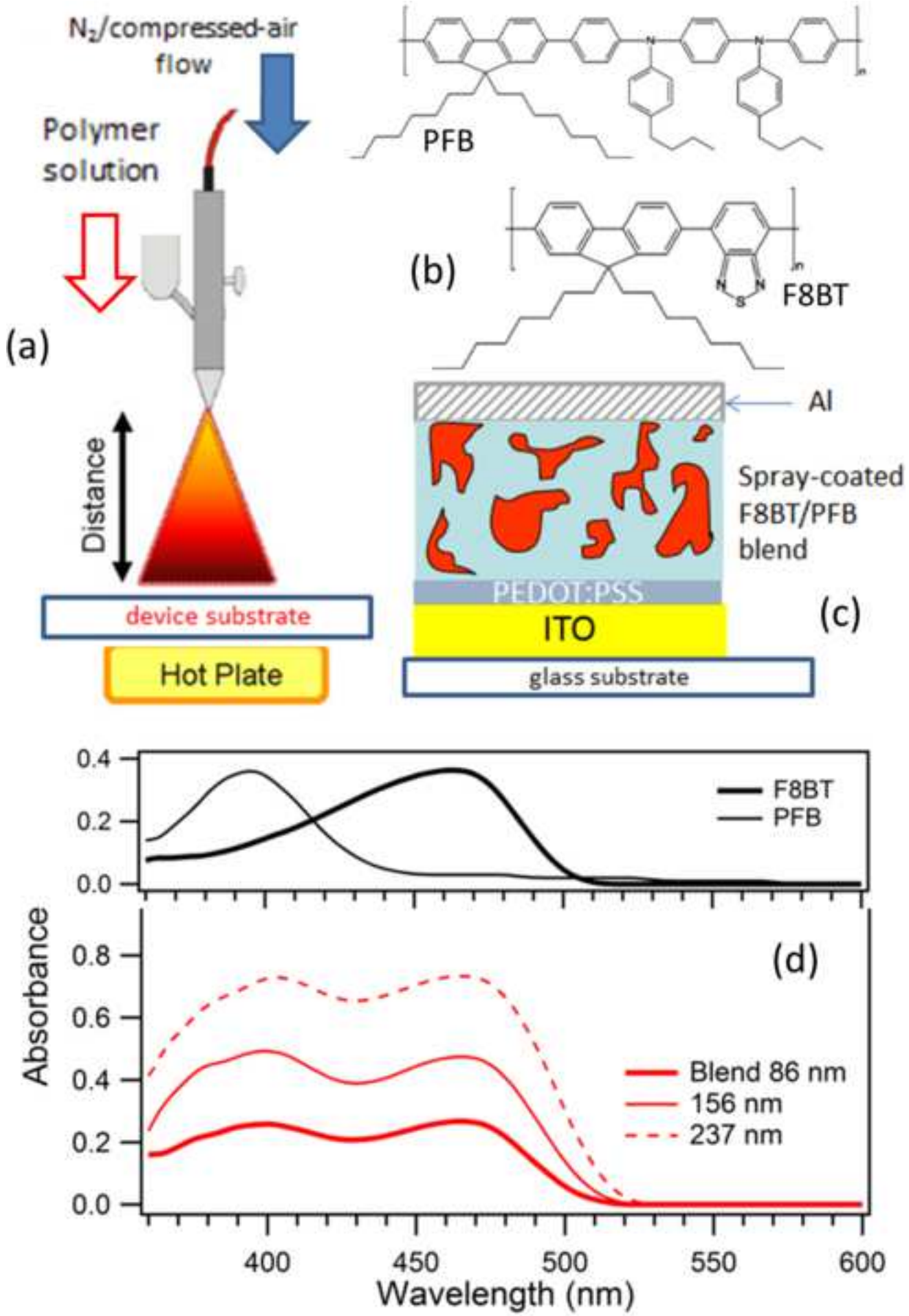

Figure 2
Click here to download high resolution image

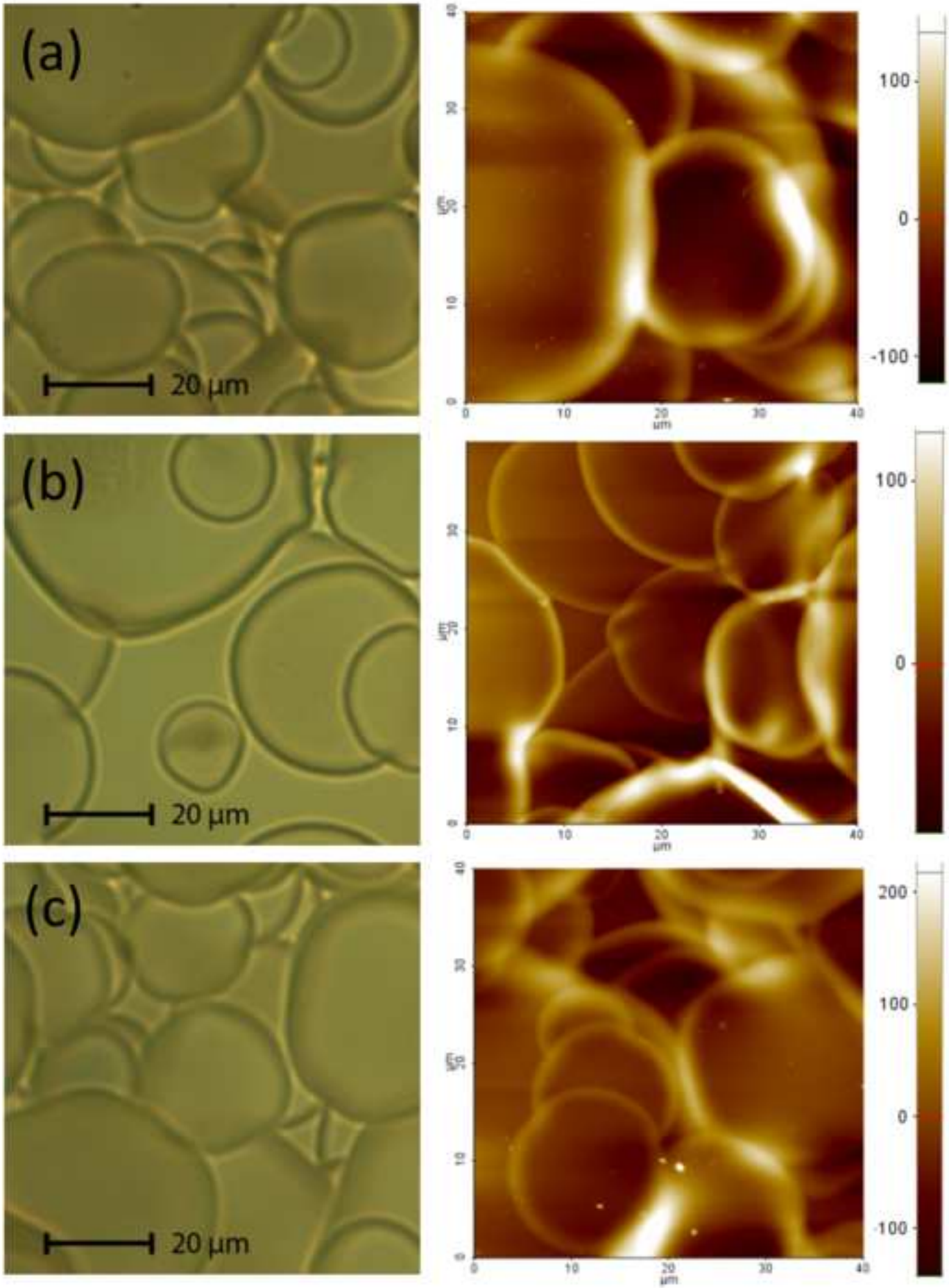

Figure 3
Click here to download high resolution image

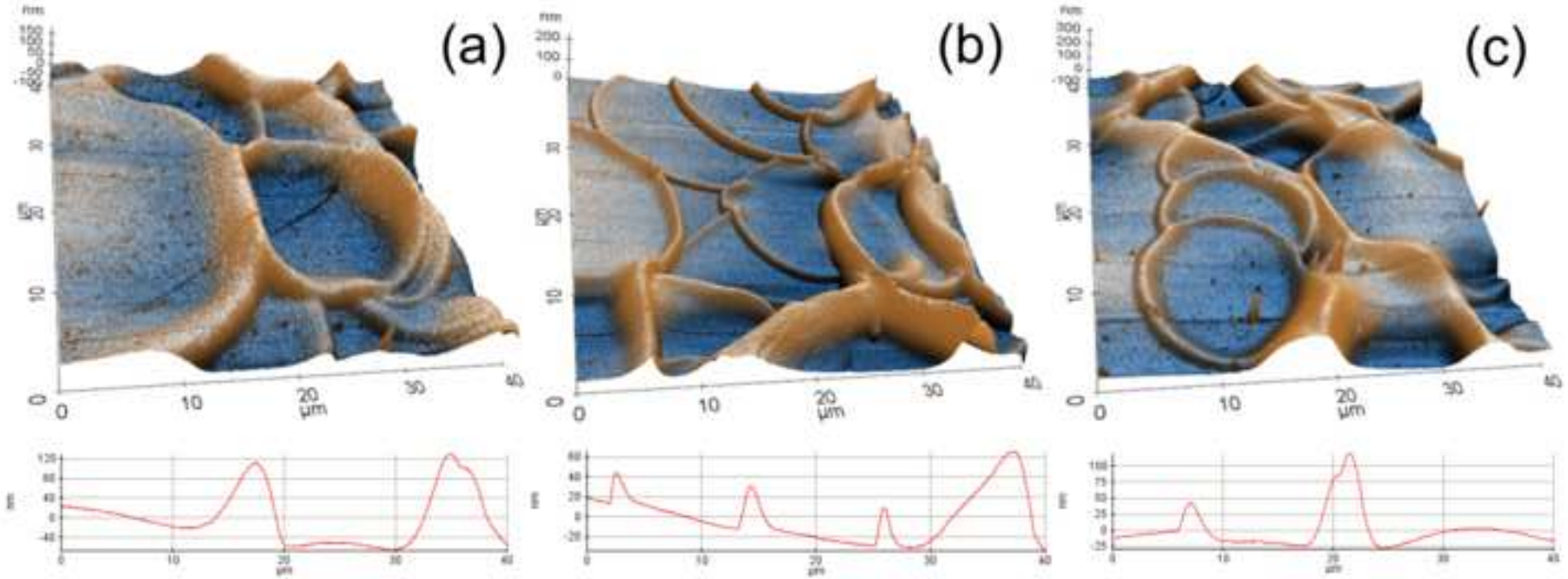

Figure 4
Click here to download high resolution image

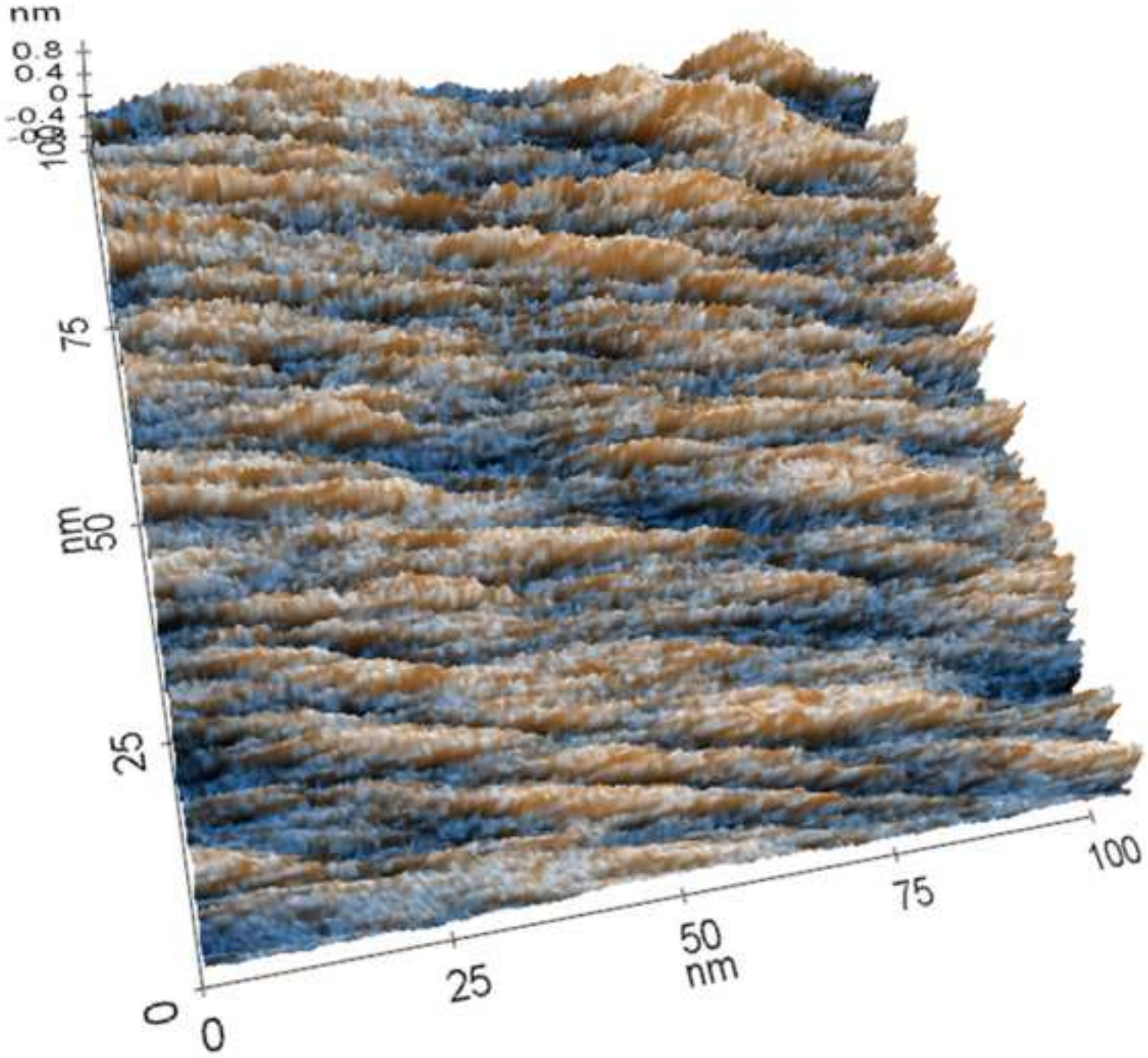

Figure 5
Click here to download high resolution image